Journal of Applied Polymer Science

Preparation of Antimicrobial Polycarboxybetaine-Based Hydrogels for Studies of Drug Loading and Release

Shouping Xu, Renchang Zeng, Jiang Cheng, Zhiqi Cai, Xiufang Wen, Pihui Pi
College of Chemistry and Chemical Engineering, South China University of Technology, Guangzhou 510640, People's Republic of China
Correspondence to: S. Xu (E-mail: cespxu@scut.edu.cn)

ABSTRACT: A series of cationic poly(*N*-isopropyl acrylamide) (PNIPAM)-*g*-poly(carboxybetaine ester) (PCBMAE) hydrogels were prepared by reversible addition–fragmentation chain-transfer polymerization with PCBMAE precursors reacting with *N*-isopropyl acrylamide in the presence of *N*,*N*′-methylene bisacrylamide. These hydrogels exhibited excellent antimicrobial activities against *Staphylococcus aureus* and could switch to nontoxic zwitterionic hydrogels after hydrolysis. Nonionic tetracycline hydrochloride (TCHC) and anionic sodium salicylate (SA) were selected to evaluate the loading capacities and release kinetics of the cationic hydrogels. We found that the loading efficiencies of TCHC in the PNIPAM-*g*-PCBMAE hydrogels were approximately twice as high as those of SA. However, the cumulative release amount of TCHC was lower than that of SA from the corresponding cationic hydrogel at 37°C. In addition, the PNIPAM-*g*-PCBMAE hydrogels exhibited accelerated release rates of both TCHC and SA with increasing content of (2-carboxymethyl)−3-acryloxyethyldimethylammonium chloride methyl ester. © 2013 Wiley Periodicals, Inc. J. Appl. Polym. Sci. **2014**, *131*, 39839.

KEYWORDS: drug-delivery systems; gels; kinetics; properties and characterization

Received 4 June 2013; accepted 9 August 2013
DOI: 10.1002/app.39839

INTRODUCTION

The poly(*N*-isopropyl acrylamide) (PNIPAM) hydrogel is one of the most popular investigated hydrogels, and it has been widely explored for drug delivery, biosensors, mass separations, and tissue engineering.[1–4] However, microbial adhesion and the formation of biofilms have been observed on the surface of the hydrogel when it was used as a biomedical material; the attachment and proliferation of microorganisms on the hydrogel surface could trigger an immune response and inflammation and result in the removal of the hydrogel. Therefore, the use of an antimicrobial hydrogel is critical for PNIPAM's application in biomaterials such as drug-release devices.

Surface modification with poly(ethylene glycol), zwitterionic sulfobetaine methacrylate,[5,6] and antimicrobial agents such as silver particles[7] has been found to be an effective method for acquiring material that reduces bacterial attachment and colonization. However, poly(ethylene glycol) tends to autoxidize in the presence of oxygen in most biochemically relevant solutions.[8] Poly(sulfobetaine methacrylate) can significantly prevent microbial colonization and biofilm formation[6] but fail to kill bacterium effectively. The construction of an antimicrobial surface with silver particles is a useful way of inhibiting microbes, but silver particles diffuse out from the hydrogel, and this leads to the weakening of its antibacterial activity.[7] It has been reported that cationic polyacrylamides bearing carboxybetaine ester groups were able to kill bacterial cells and dramatically inhibit the proliferation of fungal cells.[9–11] Polyacrylamide-bearing carboxybetaine ester groups are biocompatible materials, which can fulfill the requirement of implantable biomaterials. Herein, we synthesized a positively charged acrylic ester with a pedant group bearing carboxybetaine ester groups. It was possible to fabricate an antimicrobial hydrogel via the reaction of vinyl carboxybetaine ester with *N*-isopropyl acrylamide (NIPAM). Furthermore, the application of cationic compounds in the hydrogel was able to control the drug-release rate, prevent drug degradation, and increase the loading efficiency of the drug.[12]

In this research, reversible addition–fragmentation chain transfer (RAFT) polymerization,[13,14] a controlled/ living free-radical polymerization technique, was introduced to prepare a cationic PNIPAM-*g*-poly(carboxybetaine ester) (PCBMAE) hydrogel via two steps. The antimicrobial activities of these cationic hydrogels were investigated. Then, sodium salicylate (SA) and tetracycline hydrochloride (TCHC) were selected as drug models to study the drug uptake and the drug-release kinetics of the cationic hydrogels.

Table I. Feed Compositions and Sample Codes for the Grafted Hydrogels

	Composition[a]		
Symbol	CBMAE (g)	NIPAM (g)	MBA (g)
GG00	0	1.5	0.08
GG16	0.16	1.5	0.08
GG36	0.36	1.5	0.08
GG56	0.56	1.5	0.08

[a] The total volume of H_2O used for polymerization was 12.0 mL.

EXPERIMENTAL

Materials

Dimethylaminoethyl acrylate and methyl chloroacetate were purchased from TCI Tokyo (Japan). NIPAM, *N*-methylene bisacrylamide (MBA), ethyl ether, acetone, ammonium persulfate (APS), *N*-cyclohexyl-3-aminopropanesulfonic acid (CAPS), and SA were purchased from Aladdin Chemicals (Shanghai, China). Phosphate-buffered saline (PBS), beef extract–peptone medium (BP), and TCHC were obtained from AMRESCO. 2-(2-Carboxyethylsulfanylthiocarbonyl sulfanyl) propionic acid (TTC) was synthesized by a previously published method.[15]

Synthesis of (2-Carboxymethyl)-3-acryloxyethyldimethylammonium Chloride Methyl Ester (CBMAE)

Dimethylaminoethyl acrylate (19.63 g), methyl chloroacetate (14.11 g), and anhydrous acetone (100 mL) were added to a 250-mL, round-bottom flask. We performed the reaction by stirring the mixtures under nitrogen at 10°C. After 24 h, the white precipitate was produced at the bottom of the flask. Then, this product was taken out and washed with 100 mL of anhydrous ethyl ether twice. The precipitate was collected and dried *in vacuo* for 24 h (53% yield).

^{1}H-NMR (400 MHz, D_2O, δ): 3.32 (6H, $-N^+-CH_3$), 3.76 (3H, $-O-CH_3$), 4.00 (2H, $-CH_2-N^+$), 4.392 (2H, $N-CH_2-C=O$), 4.60 (2H, $-O-CH_2-C$), 6.00 (1H, CH=C—COO-*trans*), 6.23 (1H, =CH—COO—), 6.4 (1H, CH=C—COO-*cis*).

Preparation of PNIPAM-*g*-PCBMAE Hydrogels

Various amounts of CBMAE, APS (0.006 g), and TTC (0.0065 g) were dissolved in 4.0 mL of distilled water, and then, the mixture was added to a polymerization tube with magnetic stirring. After three freeze–pump–thaw cycles, the polymerization tube was carried out at 40°C for 24 h to prepare the CBMAE polymer with a thiocarbonylthio [—C(=S)S—R] end (PCBMAE precursors). Then, a solution of NIPAM (1.5 g), APS (0.006 g), and MBA (0.08 g) in 7 mL of deionized water was added to the polymerization tube. After the mixture was stirred for about 20 min, the reaction was conducted under nitrogen at 35°C for 24 h to produce the grafted PNIPAM-*g*-PCBMAE hydrogel. The obtained hydrogel was immersed in deionized water for 48 h to extract unreacted chemicals. These hydrogels were cut into small disks (12 mm in diameter and 3 mm in thickness) for further study. The sample codes and feed compositions of the grafted hydrogels were presented in Table I. The abbreviations GG00, GG16, GG36, and GG56 indicated that the contents of CBMAE in the PNIPAM-*g*-PCBMAE hydrogel were 0, 0.16, 0.36, and 0.56 g, respectively (Table I).

Antibacterial Activities and Safety Evaluation of the Hydrogels

The antimicrobial activities were tested and the safety evaluation of the hydrogel samples was performed according to the method reported by Cheng et al.[9] Briefly, a suspension (100 μL) of *Staphylococcus aureus* (strain 33807) was used to inoculate 20 mL of BP (20 g/L); then, the suspension was incubated at 37°C for 24 h. The culture of *S. aureus* was diluted with PBS to a concentration of 10^3 cells/mL. Some of the hydrogel samples were incubated in CAPS buffer (10 m*M*, pH 10.0) at 37°C for 48 h. Then, hydrogel disks before and after hydrolysis were transferred into separate wells of a 24-well plate. A volume of 1.0 mL of *S. aureus* suspension was added to each well. A blank control was created on a blank polystyrene surface without any hydrogel disks. The 24-well plate was sealed and incubated at 37°C for 24 h. Then, the incubated bacterial cultures were diluted thrice and spread on BP agar plates. After 18 h of incubation at 37°C, the bacterial colonies on the agar plates were counted and recorded. The antibacterial activities and safety evaluation of the gels were determined by a comparison of the bacterial colonies of the hydrogels with those of the blank control.

Characterization of Hydrogels

Fourier transform infrared (FTIR) spectroscopy with a Bruker Vector 33 spectrophotometer was used to evaluate the chemical compositions of the hydrogels in the range 4000–500 cm^{-1}. The surface areas of the dried hydrogels were measured by the nitrogen adsorption curve at 77 K with a Micromeritics TriStar II surface area analyzer. The surface area was determined with the Brunauer–Emmett–Teller (BET) equation.

Swelling Properties of the Hydrogels

The swelling behaviors of the gels were studied by mass measurement at 37°C. The swelling ratio (SR) of the hydrogel was determined as follows:

$$SR = (m_s - m_d)/m_d$$

where m_s is the mass of swollen hydrogel at a given time and m_d is the mass of dry hydrogel.

Drug Loading and Ultraviolet–Visible (UV–vis) Measurements

The freeze-dried hydrogels were immersed in a drug (SA or TCHC) aqueous solution (10 mg/mL, 10 mL) at room temperature for 48 h. After the loading equilibrium was reached, the excess solution on the surfaces was wiped off. These gels were placed at room temperature for 24 h and then dried *in vacuo* for 48 h. The loading efficiency of the drug was calculated as follows:

$$\text{Loading efficiency} = M_{drug}/M_{gel}$$

where M_{drug} is the weight of the drug encapsulated in the hydrogel and M_{gel} is the weight of the dry hydrogel.

Dried drug-loaded hydrogel (0.02 g) was soaked in 20 mL of deionized water at 37°C. After the drug entrapped in the hydrogel was completely released, the UV–vis spectrometer

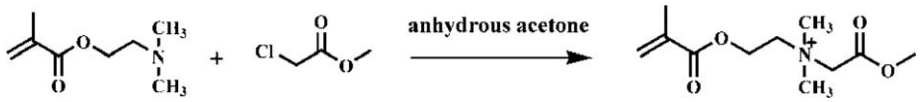

Scheme 1. Reaction scheme for the synthesis of CBMAE.

(Shimadzu UV-2450) was used to measure the absorption intensities of each drug-release solution from 250 to 350 nm.

In Vitro Release of Drugs from Hydrogels

The *in vitro* drug-release studies were carried out by the immersion of the drug-encapsulated PNIPAM-*g*-PCBMAE hydrogel into 50 mL of deionized water at 37°C. At given time intervals, 5.0 mL of the drug-release solution was taken out for concentration measurements by a UV spectrophotometer (UV-2450, Shimadzu) at 309 nm for SA and 357 nm for TCHC, respectively. A volume of 5.0 mL of fresh distilled water was simultaneously added to maintain a constant volume. All of the drug-release tests were performed in triplicate. The release kinetics was determined as follows:

$$\text{Release kinetics} = M_t / M_0$$

where M_t is the amount of drug in the release medium at a fixed time and M_0 is the amount of drug before release.

To evaluate the activity of the releasing drug model, a suspension of *Escherichia coli* with a concentration of 10^5 cells/mL was cultured first. A volume of 0.1 mL of the *E. coli* suspension was transferred into the sterilized culture tube followed by the addition of 2.0 mL of BP medium to it. Then, 1.0 mL of the drug-release solution and the fresh drug solution were added to the tub. The tube without any added drug solution was used as a control. After 24 h of incubation at 37°C, the optical density (OD) value of the incubated bacterial culture was measured by an MB-40 Enzyme-Linked Immuno Sorbent Assay (ELISA) microplate reader. The activity of the releasing drug model was estimated by comparison of the OD value of the TCHC solution with that of the control.

RESULTS AND DISCUSSION

Preparation of the PNIPAM-*g*-PCBMAE Hydrogels and FTIR Characterization

In this study, a PNIPAM-*g*-PCBMAE hydrogel was prepared by aqueous RAFT polymerization via two steps. First, CBMAE was synthesized by dimethylaminoethyl acrylate and methyl chloroacetate (Scheme 1), and it was used to prepared PCBMAE precursors with a thiocarbonylthio [—C(=S)S—R] with water-soluble TTC as a chain-transfer agent, and then, PCBMAE was reacted with NIPAM to form the grafted PNIPAM-*g*-PCBMAE hydrogel in the presence of MBA.

The FTIR spectra of the PNIPAM hydrogel and PNIPAM-*g*-PCBMAE hydrogels are displayed in Figure 1; from this, we observed that the characteristic peaks at 1530 cm^{-1} in spectra a–d were attributed to the vibration of the amide group (—CONH—) existing in the structure of NIPAM. This indicated the existence of NIPAM in both the PNIPAM hydrogel and PNIPAM-*g*-PCBMAE hydrogels. Spectra b–d show the peaks at 1752 and 1246 cm^{-1}, which were not found in spectrum a. These peaks were ascribed to the vibration of ester groups (C—O—C and —C=O, respectively) that existed in the structure of CBMA and demonstrated the hydrogel network was successfully grafted by PCBMAE. In addition, the intensity of the characteristic peak of ester group gradually became stronger with increasing CBMAE content.

Antimicrobial Activities

To evaluate the antibacterial properties of the PNIPAM-*g*-PCBMAE hydrogels, GG00, GG16, GG36, and GG56 were incubated with an *S. aureus* suspension in PBS. After 24 h of incubation at 37°C, the diluted *S. aureus* suspension was sprayed onto the growth medium. We determined the ability of the hydrogel to inhibit bacterial growth by counting the bacterial colonies on the agar plates.

As shown in Figure 2, after 24 h of incubation with GG00, numerous colonies of *S. aureus* were found on the growth medium; this was similar to the bacterial growth of the blank control and suggested that GG00 displayed no antimicrobial activity. Although little *S. aureus* colonies were observed on the agar plates after the *S. aureus* suspension was incubated with GG16, GG36, and GG56. Compared with the blank control, GG16, GG36, and GG56 presented increased antimicrobial activities of 97.9, 99.2, and 99.8% [Figure 3(a)]; these values indicated that PNIPAM-*g*-PCBMAE hydrogels with various contents of CBMAE were able to effectively inhibit the growth of bacterial cells.

PCBMAE is a switchable polymeric material with self-sterilizing properties. It was reported that the cationic polycarboxybetaine esters (PCBE) could switch to zwitterionic polycarboxybetaines upon hydrolysis, and polycarboxybetaine

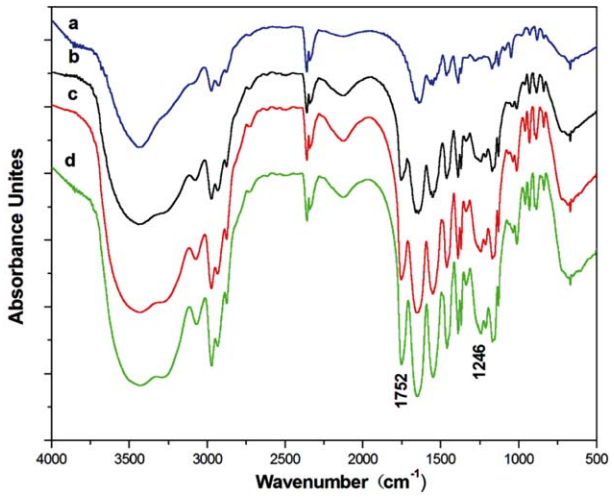

Figure 1. FTIR spectra of the (a) PNIPAM hydrogel and PNIPAM-*g*-PCBMAE hydrogels with CBMAE contents of (b) 0.16, (c) 0.36, and (d) 0.56 g. [Color figure can be viewed in the online issue, which is available at wileyonlinelibrary.com.]

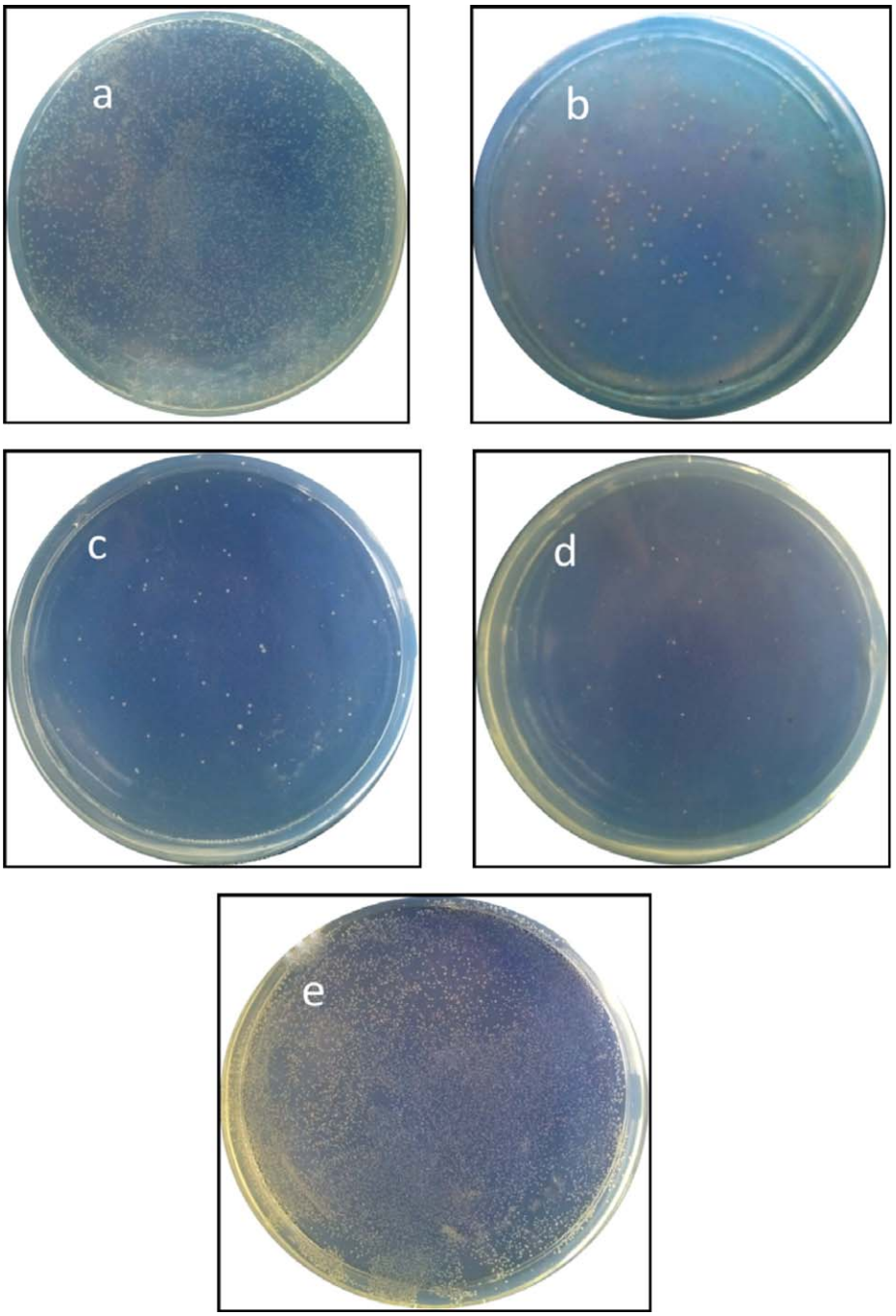

Figure 2. Photographs of the *S. aureus* colonies adhering to agar plates for (a) GG00, (b) GG16, (c) GG36, (d) GG56, and (e) a blank control. [Color figure can be viewed in the online issue, which is available at wileyonlinelibrary.com.]

hydrogels were shown to be nontoxic, biocompatible materials by their implantation into mice for 4 weeks.[16] In our study, after these hydrogels were hydrolyzed in CAPS buffer at 37°C, the live-cell percentages of GG16, GG36, and GG56 were 92.1, 91.3, and 93.5%, respectively [Figure 3(b)]; this implied that the antibacterial activities of these hydrogels almost disappeared after hydrolysis. On the other hands, the PNIPAM hydrogel proved to keep a cell viability of more than 94.0% by the 3-(4,5-dimethylthiazol-2-yl)-2,5-diphenyltetrazolium bromide (MTT) assay.[2] Therefore, we concluded that there was no toxicity for the PNIPAM-*g*-PCBMAE hydrogels after they were hydrolyzed to zwitterionic hydrogels.

Swelling Studies

Because the SR of the hydrogel had a significant effect on the drug loading and the drug-release kinetics, the swelling behaviors of GG00, GG16, GG36, and GG56 were investigated in deionized water at 37°C. From the data in Figure 4, we observed that GG56 had the largest SR of 20.2, whereas the SRs of GG00, GG16, and GG36 were 2.8, 15.1, and 17.4,

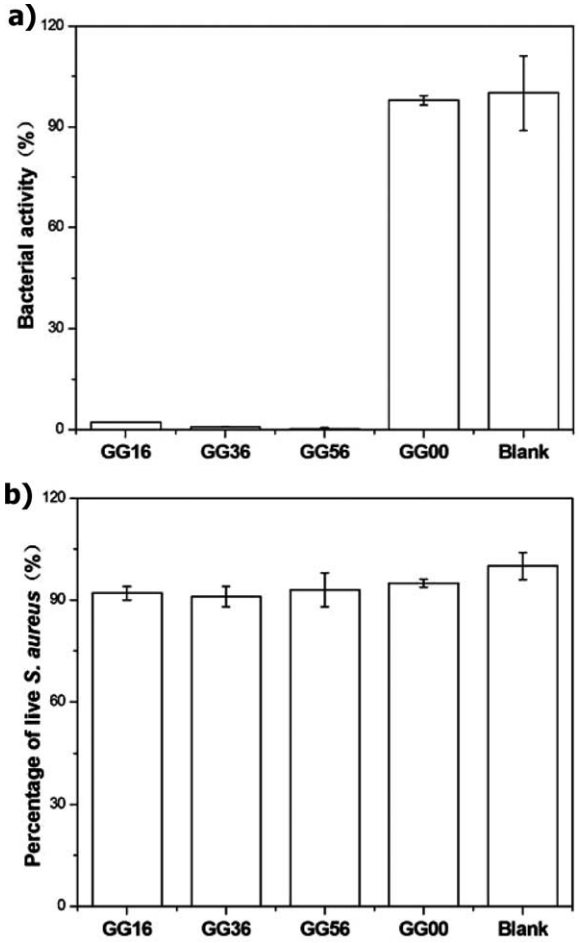

Figure 3. (a) Antimicrobial activities of the PNIPAM-*g*-PCBMAE hydrogels with different CBMAE contents against *S. aureus* in comparison with a blank control. (b) Percentage of live *S. aureus* with the PNIPAM-*g*-PCBMAE hydrogels after hydrolysis in comparison with a blank control.

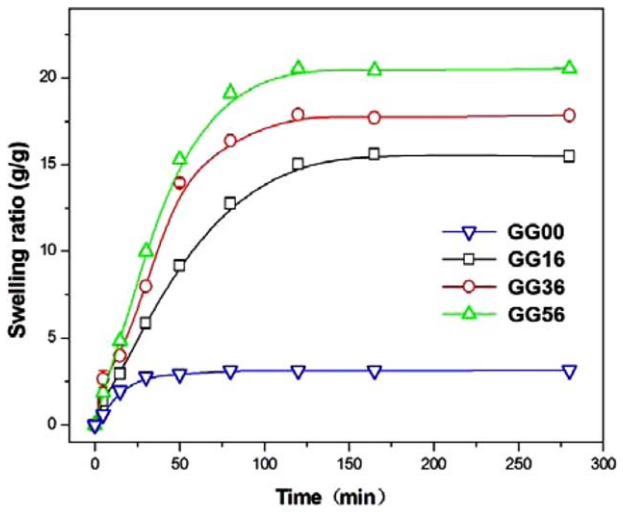

Figure 4. Swelling behaviors of the PNIPAM-*g*-PCBMAE hydrogels with different CBMAE contents as a function of time. [Color figure can be viewed in the online issue, which is available at wileyonlinelibrary.com.]

Table II. Drug Loadings of PNIPAM-*g*-PCBMAE Hydrogels with Various CBMAE Contents

	Sample code			
Drug	GG00	GG16	GG36	GG56
SA	0.058	0.114	0.123	0.165
TCHC	0.162	0.275	0.296	0.337

respectively. It suggests that the equilibrated SRs of these hydrogels increased as the content of CBMAE in the hydrogel increased. The reasons why the SRs of the hydrogels increased with different monomer contents were previously reported. For example, Singh and Pal[17] proposed that the increased SR was mainly caused by the hydrophilicity of the monomer; this could enhance the hydrophilicity of the gel network and increase the water uptake. Xiang et al.[18] considered the cross-linking density of the hydrogel to be the most important reason to the alteration of the SR. Kim et al.[19] reported that a more porous structure resulted in a higher SR because the structure with more pores provided more water channels for the adsorption of water molecules. In this study, we believe that the increase in SR from GG00 to GG56 were possibly due to the increased porosity of the gel networks, which was probably caused by the increased CBMAE contents in the hydrogels.

The BET surface areas of the hydrogels were determined by nitrogen adsorption isotherms. It is accepted that more porous materials show larger BET surface areas.[20] The BET surface areas of GG00, GG16, GG36, and GG56 were 3.247, 8.477, 9.519, and 10.008 cm^2/g, respectively; this confirmed the suggestion that the hydrogel matrix become more porous as the CBMAE content of the hydrogel increased.

Drug Loading

Two drugs, nonionic TCHC and anionic SA, were chosen to evaluate the loading efficiencies of the PNIPAM-*g*-PCBMAE hydrogels with various CBMAE contents. As shown in Table II, the drug loadings of SA in GG00, GG16, GG36, and GG56 were 0.058, 0.114, 0.123, and 0.165, respectively. We found that the loading efficiencies of the hydrogels increased from GG00 to GG56; this was in good agreement with the equilibrated SRs. These increased loading efficiencies of SA were ascribed to the increased porosity of the hydrogel networks. The loading capacities of TCHC for GG00, GG16, GG36, and GG56 were 0.162, 0.275, 0.296, and 0.337; these values were much higher than those of anionic SA in the same samples. These significant differences were possibly caused by an ionization effect between the cationic hydrogel and anionic drug molecules. In the process of drug loading, anionic SA molecules moved out of the hydrogel network more easily than the nonionic TCHC molecules; this led to a lower loading efficiency of SA.

The drug-loaded hydrogels were soaked in 20 mL of deionized water at 37°C. After the drug-release equilibrium was achieved, the UV–vis spectrometer was used to measure the absorption

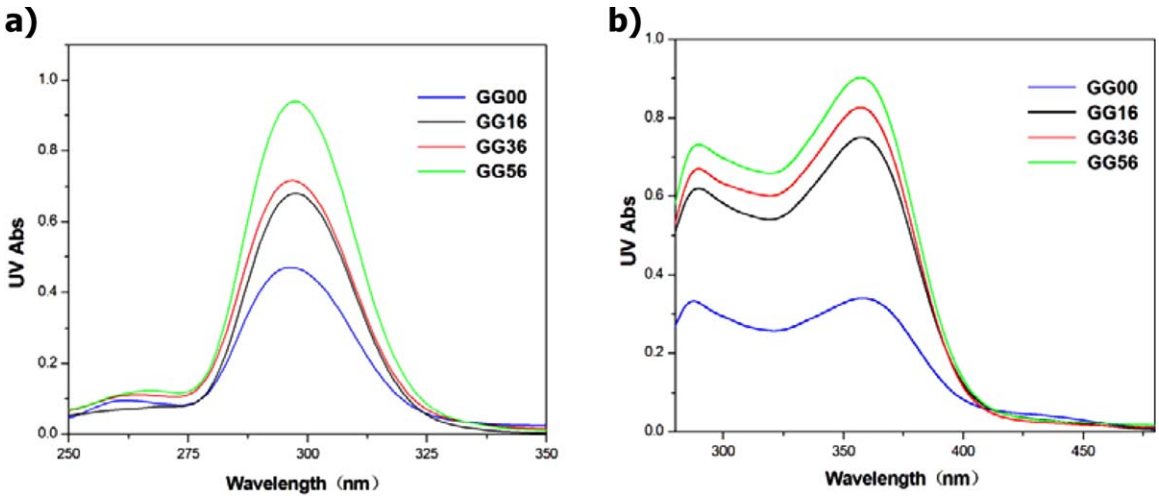

Figure 5. UV–vis absorption (Abs) spectra for (a) SA and (b) TCHC solutions. [Color figure can be viewed in the online issue, which is available at wileyonlinelibrary.com.]

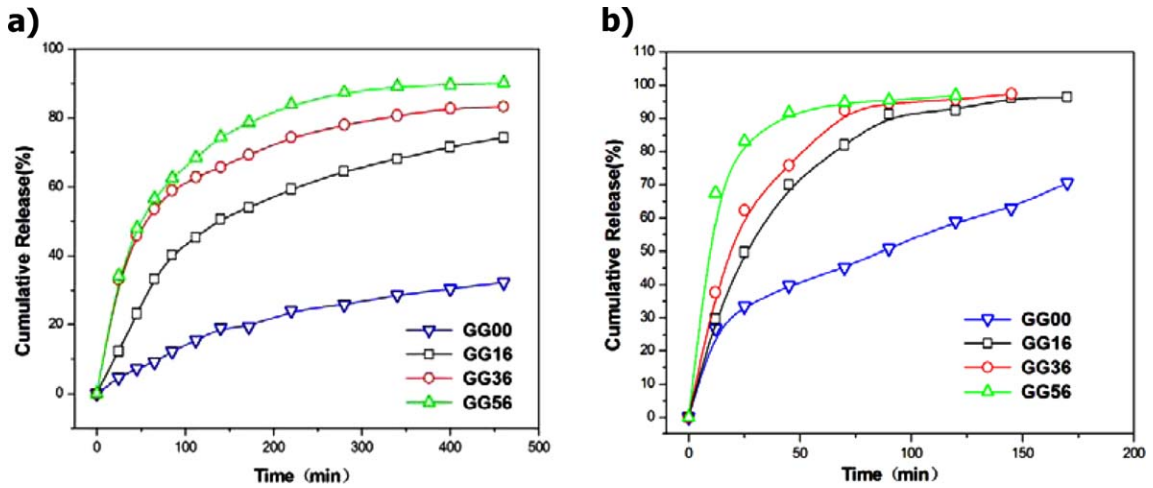

Figure 6. Cumulative amounts of (a) TCHC and (b) SA released from GG00, GG16, GG36, and GG56 at 37°C. [Color figure can be viewed in the online issue, which is available at wileyonlinelibrary.com.]

intensities of the drug solutions. As illustrated in Figure 5, the UV–vis absorption intensities for both the SA and TCHC solutions gradually became stronger from GG00 to GG56; this indicated that the loading capacities of the PNIPAM-*g*-PCBMAE hydrogels were enhanced with increasing CBMAE content of the hydrogel.

Drug-Release Studies

The drug-release kinetics from the cationic hydrogels was studied with two hydrophilic drugs, nonionic TCHC and anionic SA. The release profiles of TCHC from GG00, GG16, GG36, and GG56 are illustrated in Figure 6(a). We observed that the CBMAE content had a great influence on the cumulative release amounts of TCHC. The cumulative release of TCHC increased from 30 to 90% with increasing content of CBMAE from 0 to 0.56 g. This was because inclusion complexes formed between TCHC and the polymeric network during the drug-loading process,[4] and this internal

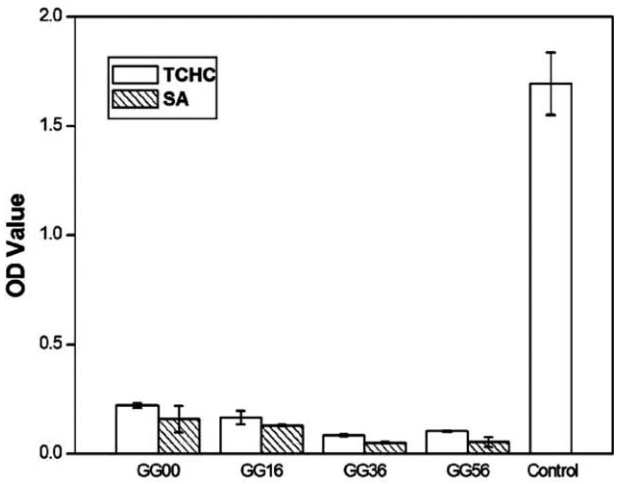

Figure 7. OD values of the drug-release solutions incubated with *E. coli* suspensions.

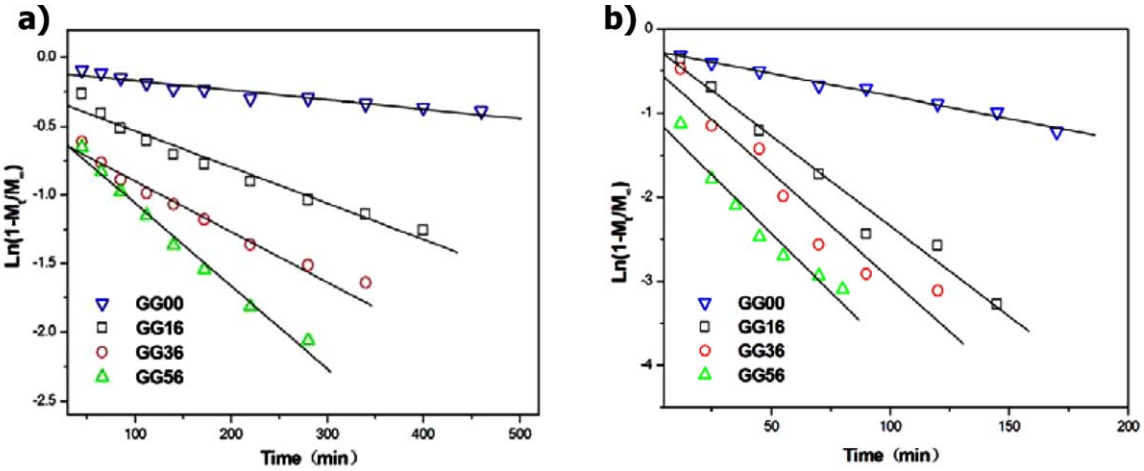

Figure 8. Plots of $\ln(1 - M_t/M_\infty)$ against t for (a) TCHC and (b) SA released from GG00, GG16, GG36, and GG56. [Color figure can be viewed in the online issue, which is available at wileyonlinelibrary.com.]

combination provided a force to prevent the TCHC molecules from releasing and resulted in a low release amount. Although the hydrogel was grafted with hydrophilic PCBMAE chains, the high hydrophilicity of PCBMAE allowed the water molecules to penetrate into the matrix and the TCHC molecules to diffuse out of the network simultaneously. With increasing content of CBMAE, the PNIPAM-*g*-PCBMAE hydrogels showed higher hydrophilicity, and this resulted in the ease of drug emigration.

Figure 6(b) illustrates the cumulative release of SA from the PNIPAM-*g*-PCBMAE hydrogels as a function of time at 37°C. We found that the anionic groups in the drug molecules significantly affected the cumulative release amount of the cationic gels. For instance, more than 92% of the loaded SA was released from GG16, GG36, and GG56; this was higher than that of TCHC. Because SA is a charged molecule, there may have been no interaction between the SA molecules and the cationic gel network because of an ionization effect. During the release process, the SA molecules were able to diffuse out of the network much more quickly than the TCHC molecules in the same time. Thus, the cumulative release amounts of the anionic drug were higher than those of the nonionic drug in the corresponding PNIPAM-*g*-PCBMAE hydrogels.

The activities of TCHC released from the hydrogels were evaluated by measurement of the OD values of the TCHC release solutions incubated with *E. coli* suspension. Generally, the increase in the OD value was attributed to the proliferation of bacterium, which reflected the low antimicrobial activity of the released drug. As shown in Figure 7, we found that the OD values for GG00, GG16, GG36, and GG56 were 0.222, 0.165, 0.084, and 0.053, respectively, whereas for the control, it was 1.693. This suggests that the TCHC released from these hydrogels still retained good activities against the bacterium. For the activity evaluation of SA release, the drug-release solution was acidized first. We observed that the OD values for these hydrogels were remarkably lower than that of the control because SA was acidized to salicylic acid, which is usually used for disinfectant. This indicated that SA still retained excellent activity after it was released from the hydrogel.

The diffusion rates of TCHC and SA from the hydrogels could be evaluated approximately by eq. (1), which can be simplified to eq. (2) by taking the first term in summation and adopting a logarithmic transformation:[12,17,21]

$$\frac{M_t}{M_\infty} = 1 - \frac{8}{\pi^2} \sum_{n=0}^{\infty} \frac{1}{(n+1)^2} \exp\left\{ -\frac{(2n+1)^2 D \pi^2}{l^2} t \right\}. \quad (1)$$

$$\ln\left(1 - \frac{M_t}{M_\infty}\right) = \ln\frac{8}{\pi^2} - \frac{D\pi^2}{l^2} t. \quad (2)$$

where M_∞ is the cumulative amount of drug released at infinite time, l is the thickness of the hydrogel, and D is the diffusion coefficient of the hydrogel, which can be obtained from the slope ($k = D\pi^2/l^2$) of the tread line by the plot of the $\ln(1 - M_t/M_\infty)$ against time (t).

According to eq. (2), the fitted regression lines of the TCHC and SA release data are presented in Figure 8 and the fitting parameters, including k, D, and the correlation coefficient (R^2), are summarized in Table III. In general, the drug-release rate of the gel was controlled by the diffusion rate of the drug. As

Table III. Fitting Parameters for the Release of TCHC and SA from the PNIPAM-*g*-PCBMAE Hydrogels with Different CBMAE Contents

Drug	CBMAE (g)	k (min^{-1})[a]	$D \times 10^4$ (cm^2/min)	R^2
TCHC	0	0.0007	2.840	0.928
	0.16	0.0025	10.142	0.980
	0.36	0.0034	13.794	0.974
	0.56	0.0060	24.342	0.987
SA	0	0.0054	21.908	0.988
	0.16	0.0215	87.225	0.978
	0.36	0.0253	102.64	0.927
	0.56	0.0280	113.60	0.948

[a] k is the slope of the linear regression.

shown in Table III, the *D* values for both TCHC and SA increased with increasing content of CBMAE of the hydrogel; this suggested that a higher CBMAE content in the hydrogel resulted in an accelerated release rate of the TCHC and SA.

CONCLUSIONS

We succeeded in preparing a cationic PNIPAM-*g*-PCBMAE hydrogel by introducing an aqueous RAFT polymerization technique. Compared to the NIPAM hydrogel, a series of PNIPAM-*g*-PCBMAE hydrogels exhibited excellent antimicrobial activities against *S. aureus* and could switch to nontoxic zwitterionic hydrogels after hydrolysis. The swelling studies showed that the equilibrium SR of the PNIPAM-*g*-PCBMAE hydrogels increased with the CBMAE content because of the increased porosity of the gel networks. In addition, the drug-loading efficiency of the cationic PNIPAM-*g*-PCBMAE hydrogel was strongly affected by the charged drug and the CBMAE content. The loading capacity of the nonionic TCHC was much higher than that of anionic SA in the corresponding PNIPAM-*g*-PCBMAE hydrogel because of the ionization effect. The drug-release tests demonstrated that the cumulative release amounts of TCHC was greatly dependent on the amount of CBMAE, whereas that of SA was not. We could finely adjust the release rate of both TCHC and SA by adjusting the CBMAE amount in the PNIPAM-*g*-PCBMAE hydrogels. Both of the drugs releasing from these hydrogels exhibited good stability in activities; this suggested it had great potential for applications in drug-release devices.

ACKNOWLEDGMENTS

This work was financially supported by the National Science Foundation of China (contract grant number 21104021 and 21176091) and the Fundamental Research Funds for the Central Universities (contract grant number 20112B0006).

REFERENCES

1. Zhao, C.; Zhuang, X.; He, P.; Xiao, C.; He, C.; Sun, J.; Chen, X.; Jing, X. *Polymer* **2009**, *50*, 4308.
2. Zhang, J.-T.; Bhat, R.; Jandt, K. D. *Acta Biomater.* **2009**, *5*, 488.
3. Zhang, X.-Z.; Wu, D.-Q.; Chu, C.-C. *Biomaterials* **2004**, *25*, 3793.
4. Zhang, J.-T.; Huang, S.-W.; Liu, J.; Zhuo, R.-X. *Macromol. Biosci.* **2005**, *5*, 192.
5. Li, G.; Xue, H.; Cheng, G.; Chen, S.; Zhang, F.; Jiang, S. *J. Phys. Chem. B* **2008**, *112*, 15269.
6. Cheng, G.; Zhang, Z.; Chen, S.; Bryers, J. D.; Jiang, S. *Biomaterials* **2007**, *28*, 4192.
7. James, C.; Johnson, A. L.; Jenkins, A. T. A. *Chem. Commun.* **2011**, *47*, 12777.
8. Zhang, Z.; Chao, T.; Chen, S.; Jiang, S. *Langmuir* **2006**, *22*, 10072.
9. Cheng, G.; Xue, H.; Li, G.; Jiang, S. *Langmuir* **2010**, *26*, 10425.
10. Cheng, G.; Xue, H.; Zhang, Z.; Chen, S.; Jiang, S. *Angew. Chem. Int. Ed.* **2008**, *47*, 8831.
11. Cao, Z.; Mi, L.; Mendiola, J.; Ella-Menye, J.-R.; Zhang, L.; Xue, H.; Jiang, S. *Angew. Chem.* **2012**, *124*, 2656.
12. Liu, J.; Li, L.; Cai, Y. *Eur. Polym. J.* **2006**, *42*, 1767.
13. Yusa, S.-I.; Fukuda, K.; Yamamoto, T.; Ishihara, K. *Biomacromolecules* **2005**, *6*, 663.
14. Rodriguez-Emmenegger, C.; Schmidt, B. V. K. J.; Sedlakova, Z.; Šubr, V.; Alles, A. B.; Brynda, E.; Barner-Kowollik, C. *Macromol. Rapid Commun.* **2011**, *32*, 958.
15. Wang, R.; McCormick, C. L.; Lowe, A. B. *Macromolecules* **2005**, *38*, 9518.
16. Zhang, Z.; Cheng, G.; Carr, L. R.; Vaisocherová, H.; Chen, S.; Jiang, S. *Biomaterials* **2008**, *29*, 4719.
17. Singh, B.; Pal, L. *Eur. Polym. J.* **2008**, *44*, 3222.
18. Xiang, Y.; Peng, Z.; Chen, D. *Eur. Polym. J.* **2006**, *42*, 2125.
19. Zhang, J.-T.; Petersen, S.; Thunga, M.; Leipold, E.; Weidisch, R.; Liu, X.; Fahr, A.; Jandt, K. D. *Acta Biomater.* **2010**, *6*, 1297.
20. Wang, Y.; Caruso, F. *Adv. Mater.* **2006**, *18*, 795.
21. Pekcan, Ö.; Erdoğan, M. *Eur. Polym. J.* **2002**, *38*, 1105.